

Poly(*p*-phenylene sulfide) Synthesis: A Step-Growth Polymerization with Unequal Step Reactivity

Darryl R. Fahey,* Harvey D. Hensley, Carlton E. Ash, and Dwayne R. Senn

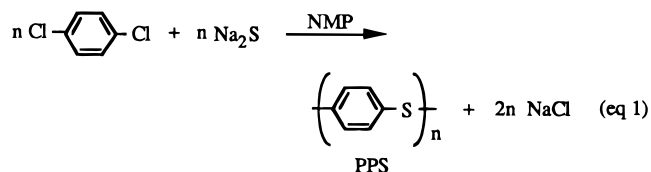
Research and Development, Phillips Petroleum Company, Bartlesville, Oklahoma 74004

Received July 12, 1996; Revised Manuscript Received November 20, 1996[®]

ABSTRACT: The anomalous responses of M_w to conversion and to comonomer stoichiometry, i.e., deviations from expected classic A–A + B–B step-growth polycondensation behavior, observed in poly(*p*-phenylene sulfide) synthesis from *p*-dichlorobenzene and sodium sulfide are shown to be a consequence of unequal rate constants for the growth steps. The polymerization is simulated by a computer model based on the step-growth polymerization concept and includes cyclization and side reactions. Rate constants and activation energies for the growth and side reactions were obtained by measurements of reaction rates of actual reaction intermediates or model compounds, while those for cyclizations were estimated.

Introduction

The anomalous features of the industrially important^{1–3} Edmonds and Hill⁴ synthesis of poly(*p*-phenylene sulfide) (PPS) from *p*-dichlorobenzene (DCB) and sodium sulfide in *N*-methylpyrrolidinone (NMP) have evoked a variety of mechanistic interpretations in recent years.^{3,5–16} Although growth of the polymer may be written as a series of conventional condensation steps, the system displays significant deviations from classic^{17,18} A–A + B–B step-growth polycondensation behavior. First, at incomplete conversions, polymer (or oligomer) yields and molecular weights are higher than expected.^{5,6,9–11,13} This feature of PPS synthesis has been demonstrated in several published experimental plots of polymer molecular weight vs extent of reaction (or conversion).^{9,10,11,13} Second, perfect 1:1 stoichiometric monomer ratios are not required to achieve high molecular weight polymer. In fact, patented process examples often disclose that the optimum ratio is typically a 1–3% molar excess of DCB over Na₂S.¹⁹ Lastly, the deceptively simple equation typically written for PPS polymerizations (eq 1) is not, in reality, the



conventional A–A + B–B polymerization system it appears to be. Instead, the NMP provides for a homogeneous reaction mixture by initially reacting with Na₂S and water to produce an equimolar mixture of sodium 4-(*N*-methylamino)butanoate (SMAB) with sodium hydrosulfide, hereafter referred to as SMAB–NaSH.¹⁵ This is a critical subtlety that must be addressed in any mechanistic discussion of PPS polymerization chemistry. Most recently, experimental studies directed toward the commercial process for PPS synthesis have led to the conclusions that the polymerization occurs by a step-growth process and that the dominant mechanism of each step is an S_NAr displacement of halide by a sulfur nucleophile.¹⁵ Implicit in this mechanism is that

the rate constants for each of the growth steps differ as a function of the aromatic ring substituents. Variations in aryl chloride reactivities in reactions proceeding by an S_NAr mechanism are well-known to be dependent upon the other ring substituents.²⁰ In fact, for PPS, predictions that rate constants for growth steps might be significantly higher than those for initiation have appeared.^{12,14,15,21}

Three significantly different mathematical models for the PPS polymerization process have been published, but the models either incorrectly assumed heterogeneous reactions between DCB and Na₂S or failed to fully incorporate an empirically determined set of rate constants for all the key growth, cyclization, and side reactions.^{14,21,22} This report presents results that more completely define the kinetics of the commercially practiced PPS polymerization process. Rate constants for the key reactions occurring during polymerization, all of which proceed by the S_NAr mechanism, have been determined. A mathematical model comprised of the equations that describe the complex dynamics of the polymerization has been incorporated into a computer program that utilizes these constants. Simulations of the polymerization with the program capture the unusual features of the PPS polymerization chemistry.

Results and Discussion

Rate Constant Determinations. Observed second-order rate constants measured for actual and model PPS growth steps are listed in Table 1. In reactions 2, 4, 6, 8, 9, and 10, subsequent substitution reactions of initial products occurred. The rate constants reported for these reactions are those for the initial substitutions. In favorable cases, rate constants for the subsequent substitutions also were determined, and those values are listed for reactions 7, 11, 12, 13, 14, and 15. In reaction 2, the initially produced arenethiol must be deprotonated to the arenethiolate anion to enable it to react with a second aryl halide (reaction 15). This deprotonation reaction was demonstrated to be rapid and not rate-limiting in an experiment in which 1 equiv of thiophenol was introduced to an NMP solution containing equivalent amounts of SMAB and DCB at 200 °C; without any induction period, the “thiophenol” reactivity toward DCB was observed to be kinetically equivalent to that of sodium benzenethiolate. In reactions 1 and 3, the initial products did not undergo

[®] Abstract published in *Advance ACS Abstracts*, January 15, 1997.

Table 1. Experimentally Determined Rate Constants for Growth Reactions^a

reaction number	sulfur reactant	aryl halide	$k, {}^b \text{M}^{-1} \text{s}^{-1}$ ($\times 10^3$)
1	SMAB–NaSH	<i>p</i> -ClC ₆ H ₄ Cl	1.43
2	SMAB–NaSH	<i>p</i> -ClC ₆ H ₄ SC ₆ H ₅	4.0
3	SMAB–NaSH	<i>p,p'</i> -ClC ₆ H ₄ SC ₆ H ₄ Cl	18.7
4	NaSC ₆ H ₅	<i>p</i> -ClC ₆ H ₄ Cl	1.75
5	NaSC ₆ H ₅	<i>p</i> -ClC ₆ H ₄ SC ₆ H ₅	6.0
6	NaSC ₆ H ₅	<i>p,p'</i> -ClC ₆ H ₄ SC ₆ H ₄ Cl	26.4
7	NaSC ₆ H ₅	<i>p,p'</i> -Cl(C ₆ H ₄ S) ₂ C ₆ H ₅ ^c	14 ^d
8	<i>p</i> -NaSC ₆ H ₄ Cl	<i>p</i> -ClC ₆ H ₄ Cl	0.78
9	<i>p</i> -NaSC ₆ H ₄ Cl	<i>p</i> -ClC ₆ H ₄ SC ₆ H ₅	3.5
10	<i>p</i> -NaSC ₆ H ₄ Cl	<i>p,p'</i> -ClC ₆ H ₄ SC ₆ H ₄ Cl	12
11	<i>p</i> -NaSC ₆ H ₄ Cl	<i>p,p'</i> -Cl(C ₆ H ₄ S) ₂ C ₆ H ₅ ^c	7.2 ^d
12	<i>p</i> -NaSC ₆ H ₄ Cl	<i>p,p',p''</i> -Cl(C ₆ H ₄ S) ₂ C ₆ H ₄ Cl ^c	12 ^d
13	<i>p</i> -NaSC ₆ H ₄ Cl	<i>p,p',p''</i> -Cl(C ₆ H ₄ S) ₃ C ₆ H ₅ ^c	7.2 ^d
14	<i>p</i> -NaSC ₆ H ₄ Cl	<i>p,p',p'',p'''</i> -Cl(C ₆ H ₄ S) ₃ C ₆ H ₄ Cl ^c	12 ^d
15	<i>p</i> -NaSC ₆ H ₄ SC ₆ H ₅ ^c	<i>p</i> -ClC ₆ H ₄ SC ₆ H ₅ ^e	5.6 ^f

^a Unless otherwise indicated, rate constants were determined by monitoring the pseudo-first-order disappearance of 0.001 00 M aryl halide in the presence of 0.100 M of the sulfur reagent at 200 °C. Reactions 2, 4, and 5 were also reported in ref 15. ^b Reported k values, in most cases, are averages of replicate measurements and are not statistically corrected for halide count. Observed rate constants sometimes varied by up to $\pm 20\%$. ^c Produced and consumed during experiment. ^d Determined by consecutive pseudo-first-order rate analysis. ^e Initial concentrations in this experiment were 0.100 M SMAB–NaSH and 0.200 M aryl halide. ^f Evaluated as the second step of a consecutive second-order reaction and determined by a graphical method to be 1.4 times the rate constant for reaction 2.

Table 2. Rate Constants for PPS Growth Steps Used in the Computer Model

reaction number	sulfur reactant	aryl halide	$k, {}^a \text{M}^{-1} \text{s}^{-1}$ ($\times 10^3$)
16	SMAB–NaSH	<i>p</i> -ClC ₆ H ₄ Cl	1.4
17	SMAB–NaSH	<i>p</i> -ClC ₆ H ₄ SNa	0
18	SMAB–NaSH	<i>p,p'</i> -ClC ₆ H ₄ SC ₆ H ₄ Cl	19
19	SMAB–NaSH	<i>p,p'</i> -ClC ₆ H ₄ SC ₆ H ₄ SNa	0
20	SMAB–NaSH	<i>p,p'</i> -Cl(C ₆ H ₄ S) _{<i>n</i>} C ₆ H ₄ Cl ^b	19
21	SMAB–NaSH	<i>p,p'</i> -Cl(C ₆ H ₄ S) _{<i>n</i>} C ₆ H ₄ SNa ^b	9.5 ^c
22	<i>p</i> -NaSC ₆ H ₄ Cl	<i>p</i> -ClC ₆ H ₄ Cl	0.78
23	<i>p</i> -NaSC ₆ H ₄ Cl	<i>p</i> -ClC ₆ H ₄ SNa	0
24	<i>p</i> -NaSC ₆ H ₄ Cl	<i>p,p'</i> -ClC ₆ H ₄ SC ₆ H ₄ Cl	12
25	<i>p</i> -NaSC ₆ H ₄ Cl	<i>p,p'</i> -ClC ₆ H ₄ SC ₆ H ₄ SNa	0
26	<i>p</i> -NaSC ₆ H ₄ Cl	<i>p,p'</i> -Cl(C ₆ H ₄ S) _{<i>n</i>} C ₆ H ₄ Cl ^b	12
27	<i>p</i> -NaSC ₆ H ₄ Cl	<i>p,p'</i> -Cl(C ₆ H ₄ S) _{<i>n</i>} C ₆ H ₄ Na ^b	6.0 ^c
28	<i>p</i> -Na(SC ₆ H ₄) _{<i>n</i>} Cl ^b	<i>p</i> -ClC ₆ H ₄ Cl	1.6 ^d
29	<i>p</i> -Na(SC ₆ H ₄) _{<i>n</i>} Cl ^b	<i>p</i> -ClC ₆ H ₄ SNa	0
30	<i>p</i> -Na(SC ₆ H ₄) _{<i>n</i>} Cl ^b	<i>p,p'</i> -ClC ₆ H ₄ SC ₆ H ₄ Cl	24 ^e
31	<i>p</i> -Na(SC ₆ H ₄) _{<i>n</i>} Cl ^b	<i>p,p'</i> -ClC ₆ H ₄ SC ₆ H ₄ SNa	0
32	<i>p</i> -Na(SC ₆ H ₄) _{<i>n</i>} Cl ^b	<i>p,p'</i> -Cl(C ₆ H ₄ S) _{<i>n</i>} C ₆ H ₄ Cl ^b	24 ^e
33	<i>p</i> -Na(SC ₆ H ₄) _{<i>n</i>} Cl ^b	<i>p,p'</i> -Cl(C ₆ H ₄ S) _{<i>n</i>} C ₆ H ₄ SNa ^b	12 ^{c,e}

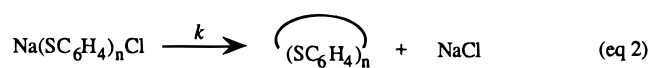
^a Values (for 200 °C) were derived from data in Table 1. ^b n is 2 or greater. ^c Assumed to be half the value of the reaction of the corresponding dichloride. ^d Interpolated from a plot of $k(p\text{-ClC}_6\text{H}_4\text{Cl})$ vs $k(p\text{-ClC}_6\text{H}_4\text{SC}_6\text{H}_5)$ in reactions with *p*-NaSC₆H₄Cl and NaSC₆H₅ with the assumption that the nucleophilicity of *p*-Na(SC₆H₄)_{*n*}Cl is equivalent to that of *p*-NaSC₆H₄SC₆H₅ (see Supplementary Figure 1). ^e Interpolated from a plot of $k(p,p'\text{-ClC}_6\text{H}_4\text{SC}_6\text{H}_4\text{Cl})$ vs $k(p\text{-ClC}_6\text{H}_4\text{SC}_6\text{H}_5)$ in reactions with *p*-NaSC₆H₄Cl and NaSC₆H₅ with the assumption that the nucleophilicity of *p*-Na(SC₆H₄)_{*n*}Cl is equivalent to that of *p*-NaSC₆H₄SC₆H₅ (see Supplementary Figure 2).

subsequent substitutions despite the presence of excess SMAB–NaSH reagent. In these cases, the initially produced chloroarylthiolates (after rapid deprotonation) were deactivated toward a second nucleophilic displacement of the remaining chloride due to the negative charge on the molecules. It is worth noting in Table 1 that not only are aryl halide reactivities influenced by substituent effects but also are sulfur anion nucleophilicities. Furthermore, this effect can be transmitted beyond the first phenyl group.

On the basis of the experimental results presented in Table 1, second-order rate constants for the key generic polymer growth reactions have been assigned and are listed in Table 2. Reactions 17, 19, 23, 25, 29, and 31 are assigned rate constant values of zero because (1) the *p*-chloro group in NaSC₆H₄Cl was observed to be unreactive toward sulfur nucleophiles in reactions 1, 8, 9, and 10, and (2) the *p*-chloro group in NaSC₆H₄SC₆H₄Cl was observed to be unreactive toward a sulfur nucleophile in reaction 3. Statistical corrections for the halide count and two approximations have been made. The first approximation is that the nucleophilicity of

NaSC₆H₄SC₆H₄Cl is equal to that of NaSC₆H₄SC₆H₅. The second is that the rate constants for the reactions of higher oligomers (e.g., reactions in Table 2 where $n > 2$) will be invariant. This latter assumption is reasonable considering comparisons within reaction sets 10, 12, and 14 and 11 and 13. This is generally regarded as a characteristic trait of condensation polymerizations.^{17,18,23}

Cyclic oligomers are produced during PPS synthesis,^{24,25} and an analysis of the material extracted from a recovered PPS product showed the following amounts of cyclic oligomers (SC₆H₄)_{*n*} relative to the whole PPS product: (n values): (4) 0.05, (5) 0.44, (6) 0.22, (7) 0.65, (8) 0.82, (9) 0.38, (10) 0.21, (11) 0.14, (12) 0.10, and (13) 0.05 wt %. These cyclic oligomers can be formed by intramolecular condensations of Na(SC₆H₄)_{*n*}Cl intermediates, where $n > 3$ (eq 2). To account for the



production of cyclic oligomers during PPS synthesis in

Table 3. Rate Constants for Intramolecular Cyclization Reactions Used in the Computer Model

reaction number	reaction intermediate	$k, ^a \text{M}^{-1} \text{s}^{-1}$ ($\times 10^5$)
34	<i>p</i> -Na(SC ₆ H ₄) ₄ Cl	1.7
35	<i>p</i> -Na(SC ₆ H ₄) ₅ Cl	14
36	<i>p</i> -Na(SC ₆ H ₄) ₆ Cl	20
37	<i>p</i> -Na(SC ₆ H ₄) ₇ Cl	23
38	<i>p</i> -Na(SC ₆ H ₄) ₈ Cl	15
39	<i>p</i> -Na(SC ₆ H ₄) ₉ Cl	14
40	<i>p</i> -Na(SC ₆ H ₄) ₁₀ Cl	8.4
41	<i>p</i> -Na(SC ₆ H ₄) ₁₁ Cl	5.0
42	<i>p</i> -Na(SC ₆ H ₄) ₁₂ Cl	3.0
43	<i>p</i> -Na(SC ₆ H ₄) ₁₃ Cl	1.8
44	<i>p</i> -Na(SC ₆ H ₄) ₁₄ Cl	1.1
45	<i>p</i> -Na(SC ₆ H ₄) ₁₅ Cl	0.7

^a For 200 °C.**Table 4. Experimentally Determined Rate Constants for Side Reactions^a**

reaction number	nucleophilic reactant	aryl halide	$k, ^b \text{M}^{-1} \text{s}^{-1}$ ($\times 10^4$)
46	SMAB	<i>p</i> -ClC ₆ H ₄ Cl	3.4
47	SMAB	<i>p,p'</i> -ClC ₆ H ₄ SC ₆ H ₄ Cl	19

^a Rate constants were determined by monitoring the pseudo-first-order disappearance of 0.001 00 M aryl halide in the presence of 0.100 M of SMAB at 270 °C. ^b Reported k values are averages of replicate measurements and are not statistically corrected for halide count.

a computer model, differential equations for the cyclization reactions in eq 2 must be incorporated in the model (vide infra). The first-order rate constants for the cyclization reactions are needed and, ideally, should be determined experimentally. However, the required Na(SC₆H₄)_{*n*}Cl compounds are not available. Therefore, rate constants for the cyclization reactions (for *n* = 4–13) were obtained through trial and error runs of the computer model. This procedure assumed that the cyclic oligomers were produced solely by intramolecular condensations of the Na(SC₆H₄)_{*n*}Cl intermediates. Rate constant values for the cyclization reactions initially were assumed, and the computer model was allowed to predict reaction outcomes. The process was repeated varying the rate constant values until the predicted cyclic oligomer yields accurately matched those measured experimentally. The first-order rate constant values that provided accurate predictions are listed in Table 3.

Another class of reactions required for a computer modeling effort are side reactions that occur during the PPS polymerization. Aryl chlorides are consumed in the presence of SMAB in a process that competes with the polymer growth steps. Rate constants for these side reactions were determined by following the disappearances of DCB and bis(4-chlorophenyl) sulfide in the presence of SMAB. Because these reactions are very slow at 200 °C, measurements were performed from 240 to 280 °C. The results at 270 °C are reported in Table 4. Extrapolations to 200 °C from Arrhenius plots yield the rate constants in Table 5.

Arrhenius activation energies were determined for selected growth steps over 200–240 °C and for side reactions over 240–280 °C. The results are reported in Table 6.

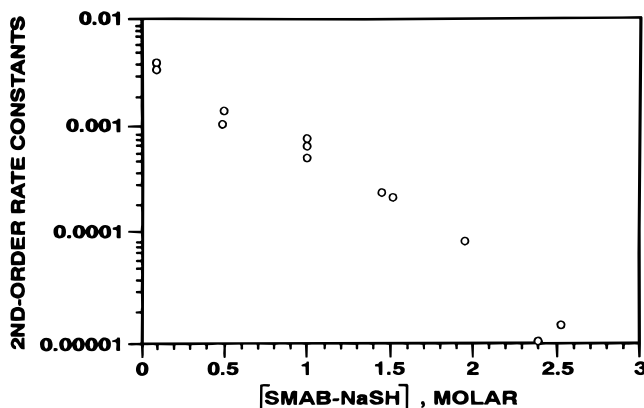
Curiously, reaction rate constants for growth steps involving SMAB–NaSH, 1 and 3, were found to be dependent upon “concentration”. This observation is believed to be a function of changing the character of the reaction medium as the reagent concentrations were

Table 5. Rate Constants for Side Reactions Used in the Computer Model

reaction number	nucleophilic reactant	aryl halide	$k, ^a \text{M}^{-1} \text{s}^{-1}$ ($\times 10^6$)
48	SMAB	<i>p</i> -ClC ₆ H ₄ Cl	1.4
49	SMAB	<i>p</i> -ClC ₆ H ₄ SNa	0
50	SMAB	<i>p,p'</i> -Cl(C ₆ H ₄) _{<i>n</i>} C ₆ H ₄ Cl ^b	7.9
51	SMAB	<i>p,p'</i> -ClC ₆ H ₄ SC ₆ H ₄ SNa	0
52	SMAB	<i>p,p'</i> -Cl(C ₆ H ₄) _{<i>m</i>} C ₆ H ₄ SNa ^b	4.0 ^c

^a Values (for 200 °C) were derived from data in Tables 4 and 6.^b *n* is 1 or greater, and *m* is 2 or greater. ^c Assumed to be half the value of the reaction of the corresponding dichloride.**Table 6. Experimentally Determined Arrhenius Activation Energies**

reaction number	sulfur reactant	aryl halide	E_a , kcal/mol
1	SMAB–NaSH	<i>p</i> -ClC ₆ H ₄ Cl	24.4
3	SMAB–NaSH	<i>p,p'</i> -ClC ₆ H ₄ SC ₆ H ₄ Cl	23.7
8	<i>p</i> -NaSC ₆ H ₄ Cl	<i>p</i> -ClC ₆ H ₄ Cl	26
10	<i>p</i> -NaSC ₆ H ₄ Cl	<i>p,p'</i> -ClC ₆ H ₄ SC ₆ H ₄ Cl	21
4	NaSC ₆ H ₅ ^a	<i>p</i> -ClC ₆ H ₄ Cl	26.9
6	NaSC ₆ H ₅ ^a	<i>p,p'</i> -ClC ₆ H ₄ SC ₆ H ₄ Cl	21
46	SMAB	<i>p</i> -ClC ₆ H ₄ Cl	40
47	SMAB	<i>p,p'</i> -ClC ₆ H ₄ SC ₆ H ₄ Cl	40

^a Model sulfur reagent for *p*-Na(SC₆H₄)_{*n*}Cl.**Figure 1.** Influence of SMAB–NaSH concentration on observed second-order rate constants ($\text{M}^{-1} \text{s}^{-1}$) for reaction with DCB in NMP at 200 °C.

varied. This is particularly true since SMAB–NaSH and the sodium arenethiolate intermediates should be regarded as “salts”.¹⁵ Rates of reactions occurring by the S_NAr mechanism are extremely sensitive to the solvent, sometimes varying several orders of magnitude with changes in solvent, dipolar aprotic solvents being the optimum.^{26–28} Small changes in the reaction medium would therefore be expected to affect reaction rates significantly. Commercial polymerizations are conducted at high concentrations, conditions where the solvation of salts and intermediates are clearly not optimum. A plot of the influence of SMAB–NaSH concentration on the rate constant for the reaction of SMAB–NaSH with DCB is displayed in Figure 1.

Computer Modeling. On the basis of the step polymerization concept and the rate constant data from Tables 2, 3, and 5, a computer model of the polymerization was constructed that considers all possible combinations of polycondensation reactions. Because an infinite set of differential equations is necessary for normal modeling, the mathematics was simplified by lumping,²⁹ i.e., reducing the problem to a finite set of equations that describe the first three moments³⁰ of the chain length distribution of a polymer. Numerical integration of the system of differential equations for

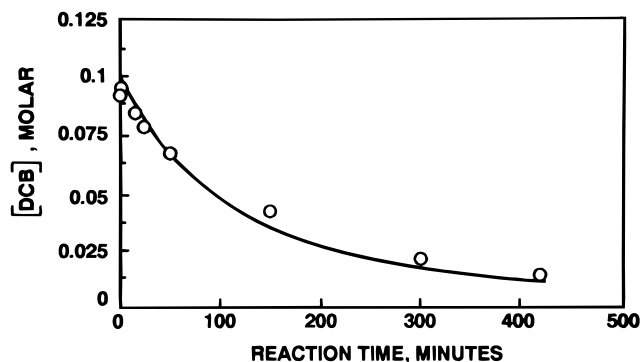


Figure 2. DCB consumption during a 200 °C polymerization: computer predicted (solid line), experimentally determined (○).

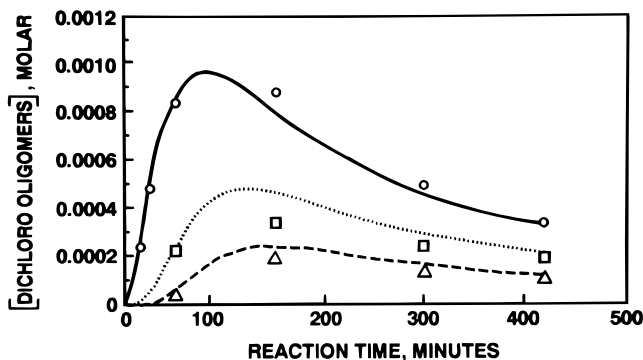


Figure 3. Dichloro oligomer concentrations during a 200 °C polymerization: computer predicted p,p' -ClC₆H₄SC₆H₄Cl (solid line), experimentally determined (○); computer predicted p,p',p'' -Cl(C₆H₄S)₂C₆H₄Cl (dotted line), experimentally determined (□); computer predicted p,p',p'',p''' -Cl(C₆H₄S)₃C₆H₄Cl (dashed line), experimentally determined (△).

the moments of lumped polymer species was achieved using a commercially available computer program.³¹ The variability of rate constants with temperature and "concentration" was also incorporated. Tracking of monomers, initial oligomers, cyclic oligomers, molecular weight, and polymer yields under various reaction conditions can be simulated.

PPS computer model predictions of the disappearance of DCB monomer and the appearance of initial intermediates were compared to concentrations experimentally observed in a PPS polymerization that was deliberately designed to be slow in rate to allow sampling and analysis of the reaction mixture during the early stages of the polymerization. Experimentally determined concentrations of DCB and several oligomers are shown at various time intervals in Figures 2 and 3. Computer-predicted concentrations for these compounds are shown as solid curves. The correlations in these figures demonstrate that the model reasonably predicts monomer disappearance and oligomer concentrations early in the reaction.

As previously mentioned, the molecular weight of the PPS polymer increases more rapidly as a function of reaction conversion than is expected for classic A-A + B-B polycondensations. The computer model predictions also exhibit this deviation from the prediction for classic A-A + B-B polycondensation behavior.^{18,32} Weight-average molecular weight growth as a function of DCB conversion is shown in Figure 4 for the PPS model, the classic theory, and for experimental data obtained in our laboratories. While plots of M_w/M_n ratios vs conversion are also of interest, reliable M_n values for PPS polymers are not available from the

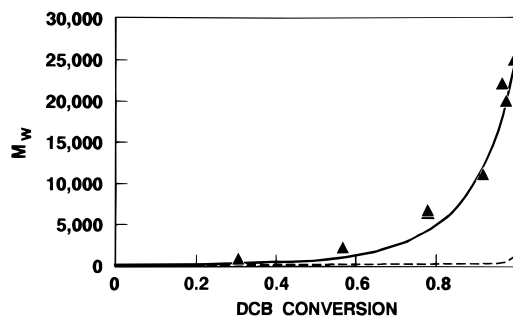


Figure 4. Development of weight average molecular weight (M_w) during polymerization for PPS synthesis from 1.00 mol of SMAB-NaSH and 1.01 mol of DCB: experimentally determined (△), PPS model prediction (solid line), classic step-growth A-A + B-B polycondensation behavior (dotted line).

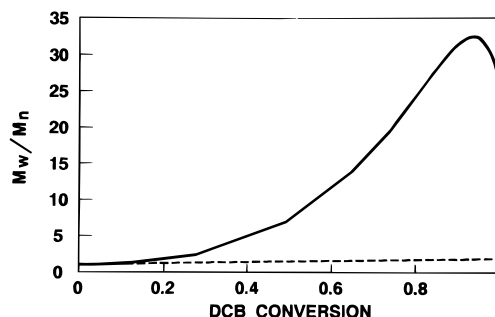


Figure 5. Ratio of M_w to M_n as a function of DCB conversion for the polymerization described in the caption to Figure 4: PPS model prediction (solid line), classic step-growth A-A + B-B polycondensation behavior (dotted line).

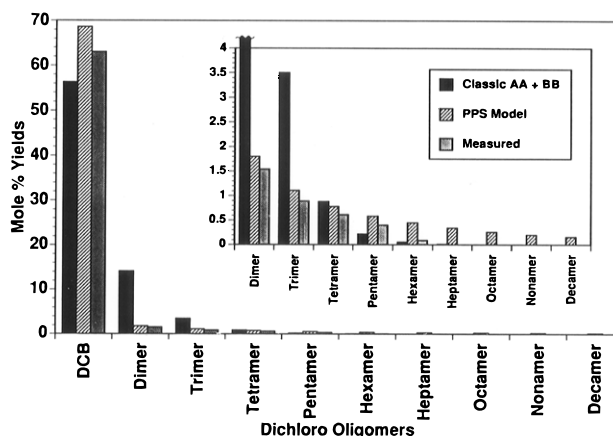


Figure 6. Comparisons of product distributions from the reaction of a 4:1 molar ratio of DCB to SMAB-NaSH: predicted for a classic step-growth A-A + B-B polycondensation, predicted by the PPS model, and experimentally measured (see experimental section for measurement limitations). The inset is an expansion of a portion of the plot.

current GPC analysis method. Despite the absence of experimental data, a comparison of the PPS model predicted M_w/M_n ratio vs DCB conversion with that for classic A-A + B-B condensation polymerizations is presented in Figure 5. The extraordinary behavior predicted by the PPS model in Figure 5 results from a rapid increase in M_w , but not M_n , during the first 90% of DCB conversion. As the polymerization continues, M_n begins to increase more rapidly than M_w .

Comparisons of predicted vs experimentally determined individual oligomer yields obtained from a polymerization containing 300% excess DCB (4:1 mole ratio of DCB to SMAB-NaSH) appear in Figure 6. First, the data set predicted by the PPS computer model

is very different from that for a classic $A-A + B-B$ condensation polymerization. The former predicts significant yields of dichloro oligomers well beyond the pentamer, while the latter does not. The contributions of higher mers are extremely significant when considered on a total product weight basis. Second, the experimental data, which are valid only up to the dichloro pentamer due to solubility limitations, are in quite good agreement with the PPS model prediction. In the experiment, only 93% of the theoretical yield was recovered. Accordingly, the measured yields are systematically slightly lower than the PPS model prediction. Although the insolubility of the dichloro hexamer and higher mers prevented their reliable yield determinations, mers up to the dichloro heptadecamer were detected by laser desorption–Fourier transform mass spectrometry analysis of the solid product mixture.

Conclusions. The unusual features displayed in PPS polymerizations are accounted for in terms of a step-growth polymerization with unequal rate constants for the key polymer growth steps. The polymer growth steps proceed by ionic S_NAr reactions with the rate constant for each reaction dependent upon the electronic influences of substituents. These reactivity differences are manifested in both the sulfur nucleophiles and the aryl chloride electrophiles. Computer simulations of the polymerization based upon these reactivity differences provide good correlations with experimental data for monomer consumption, transient oligomer concentrations, and molecular weights of the final polymer. It is therefore unnecessary to propose radical or other more complex mechanisms for the condensation of DCB and Na_2S in NMP. Other examples where step-growth polymerization with unequal step reactivity have been recognized are poly(phenylene ether sulfone) and a poly(arylene sulfone) syntheses.^{33,34,35} These examples share a commonality with PPS synthesis in that the polycondensation steps involve nucleophilic substitutions of aryl halides.

Experimental Section

Most commercially available compounds were used as received. NMP and thiophenol were distilled before use. Sodium benzenethiolate and sodium 4-chlorobenzenethiolate were prepared by dissolving equimolar amounts of NaOH and the appropriate thiophenol in methanol under argon and evaporating the solution to dryness. The thiols and their salts, NaSH, and Na_2S are susceptible to air oxidation, so they were handled under argon or nitrogen. SMAB–NaSH¹⁵ for kinetics experiments was prepared following the procedure discussed below under Preparative Polymerizations. It was not isolated from its NMP solutions but was used directly in the kinetic experiments. SMAB was synthesized by heating NaOH/ H_2O in NMP.³⁶ The syntheses of 1-chloro-4-(phenylthio)benzene and 1,4-bis(phenylthio)benzene were described previously.¹⁵

Special instrumentation was used in most of the polymer characterizations. Molecular weight analyses were performed on a specially constructed high temperature gel permeation chromatography (GPC) instrument, utilizing a Waters Model 6000A HPLC pump, connected to a Tracor Model 945 flame ionization detector (FID) with a modified application nozzle. The instrument is patterned from Kinugawa's³⁷ modification of Stacy's³⁸ method. Two Shodex AT-80 M/S mixed-bed columns were used as the stationary phase, and 1-chloronaphthalene was the mobile phase. The columns and detector were operated at 220 °C. Reliable M_n values are not obtained in this analysis because the sensitivity of the FID drops sharply below a molecular weight of 1000 and because of an increase in the tailing of the signal as the columns age. The GPC molecular weight values have an estimated uncertainty of $\pm 10\%$ and are based on universal calibration with polystyrene

standards using the Kuhn–Mark–Houwink–Sakurada constants reported by Stacy.³⁸ The experimental M_w values reported in Figure 4 were corrected from the GPC-determined values by including unreacted monomer. Extractable PPS oligomer analyses by nonaqueous reverse-phase high performance liquid chromatography (HPLC) was accomplished on a Hewlett-Packard 1090 liquid chromatograph equipped with a photodiodearray UV detector. Separations were performed using μ -Bondapak C-18 columns and CH_3CN/CH_2Cl_2 for the mobile phase. Laser desorption–Fourier transform mass spectrometry (LD–FTMS) was performed on a Nicolet 2000 Fourier transform mass spectrometer interfaced with a Ta-chisto 216 pulsed carbon dioxide laser. NMR spectra were obtained on a JEOL JNM-GX270 FT-NMR spectrometer fitted with a high-temperature, high-resolution ^{13}C probe custom built by Doty Scientific. Details of this equipment and its operation are reported elsewhere.³⁹

Apparatus. Rate studies and polymerizations were performed in Autoclave Engineers 300-mL and 1-L autoclaves constructed of 316 stainless steel or titanium metallurgies. Each reactor was equipped with a mechanical stirrer, a thermowell, a gas outlet, a gas/liquid inlet, and, in most cases, a sampling tube. Pressurized vessels connected in series were used to add coreactants and additional solvent to the autoclave to initiate reactions. Reactor temperatures were controlled to within ± 2 °C (usually ± 1 °C) following initial excursions when adding coreactants.

Rate Studies. A typical pseudo-first-order kinetic experiment is described. A 300-mL autoclave was charged with 2.50 g (15.0 mmol) of sodium 4-chlorobenzenethiolate and 117 g of NMP under a flow of argon. The apparatus was assembled and flushed with argon, and the temperature of the autoclave was increased to a few degrees higher than the desired run temperature. A deaerated, heated solution of 0.0371 g (0.150 mmol) of bis(4-chlorophenyl) sulfide and 0.15 g of biphenyl in 15 g of NMP was added from the first charge vessel. Immediately thereafter, 15 g of deaerated heated NMP was added from the second vessel through the first, and the autoclave pressure was increased to 300 psig with argon. About 15 s elapsed during these operations and the temperature would dip several degrees below the set point. At preselected intervals, 3-mL samples were withdrawn through the sampling tube (discarding a 1–2 mL forerun) under argon. Later, the pH of each sample was adjusted to 4.0 with aqueous HCl followed by extraction (3 \times) with ether. The three ether extracts were combined and analyzed by GC. Contact of the samples with air occurred only during the ether extraction process.

GC analyses were performed on a 6 ft \times 0.25 in. (3 mm i.d.) glass column packed with 3% OV-1 on 80/100 Chromosorb W-HP that was temperature programmed from 75 to 350 °C. Peak identities were assigned by GC/MS and in most cases by spiking with authentic samples. Component concentrations were calculated on the basis of peak areas relative to the internal standard (biphenyl) with corrections for relative detector responses.

Preparative Polymerizations. A general procedure is described. Into a 1-L autoclave was charged 93.3 g (1.00 mol) of NaSH hydrate, 40.4 g (1.01 mol) of NaOH, and 247.8 g of NMP. The autoclave was closed and flushed with nitrogen. The autoclave was heated to 155 °C, the vent tube was opened, and a slow flow of nitrogen was passed through the autoclave as the temperature was increased 1 °C/min to 210 °C to dehydrate the mixture. The vent was closed, and the temperature of the autoclave was adjusted to 205 °C. This was followed by the addition of 148.5 g (1.01 mol) of DCB and 99.0 g of NMP. Polymerizations were conducted for 3 or 6 h at 200, 220, or 240 °C, after which the reactor was cooled quickly.

The product was thoroughly stirred, and a 10-g portion of the crude product was combined with 20 g of 2-propanol. The latter mixture was blended and filtered, and the filtrate was subjected to GC analysis to determine residual DCB content. The DCB determined by this method was then expressed in terms of conversion where DCB conversion = (DCB charge – DCB residue)/(DCB charge). The PPS polymer was recovered by blending the product with water and adjusting the pH to 4

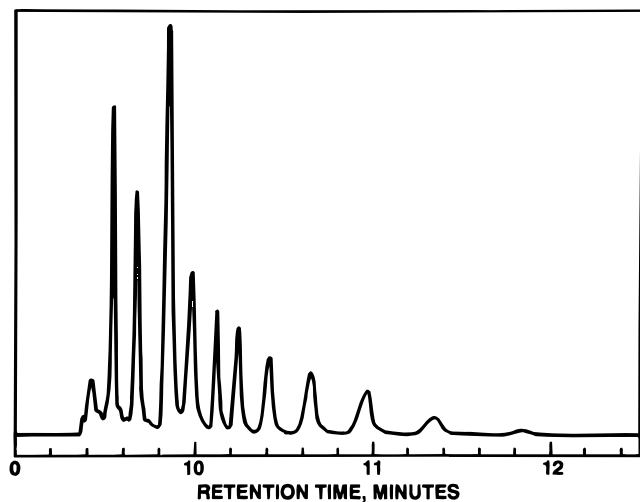


Figure 7. HPLC chromatogram of a CH_2Cl_2 extract of PPS that had been percolated through both acid-washed and base-washed aluminas. The components are cyclic PPS oligomers from the tetramer to the tridecamer.

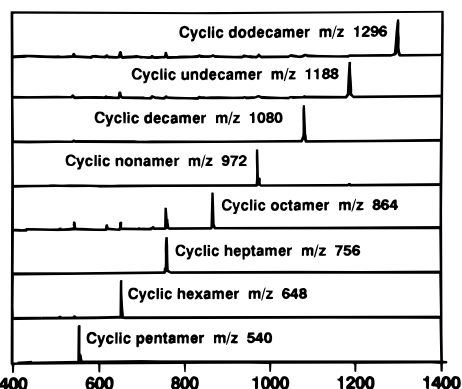


Figure 8. LD-FTMS of cyclic PPS oligomers isolated by preparative HPLC. The numerical values shown are atomic mass units.

with hydrochloric acid. The solids were filtered and washed six times with 80 °C deionized water and then dried at 100 °C in a vacuum oven.

Polymerization with 300% Excess DCB. A 1-L autoclave was charged with 89.00 g (0.700 mol) of NaSH hydrate (44%), 28.28 g (0.707 mol) of NaOH, and 225.0 g of NMP. The autoclave was then closed and flushed with nitrogen. After dehydration as in the preceding procedure, the autoclave was charged with 411.61 g (2.80 mol) of DCB and 244.0 g of NMP. Polymerization was conducted at 265 °C for 3 h, after which the reactor was cooled slowly.

The product was slurried with 2 L of water, filtered, and washed with an additional 2 L of water. The filter cake was then slurried with 1.5 L of ether and filtered. The filtrate was collected and dried with MgSO_4 , and the solvent was removed by rotary evaporation. This material was recombined with the ether insoluble material and was air-dried overnight. The recovered material weighed 356.81 g (93% of theoretical yield based on 100% conversion of SMAB-NaSH). A combination of GC and HPLC analyses of the thoroughly blended mixture provided the results reported in Figure 6.

Oligomer Analysis during Polymerization. A 300-mL autoclave was charged with 1.95 g (15.0 mmol) of Na_2S hydrate (60%) and 115 g of NMP under a flow of argon. The apparatus was assembled and flushed with argon. The autoclave was heated to 155 °C, the vent tube was opened, and a slow flow of argon was passed through the autoclave as the temperature was increased 1 °C/min to 210 °C to dehydrate the mixture. The vent was closed and the temperature of the autoclave was adjusted to 205 °C. A deaerated, heated solution of 2.205 g (15.0 mmol) of DCB and 1.50 g of biphenyl in 15 g of NMP

was added from the first charge vessel. Immediately thereafter, 15 g of deaerated, heated NMP was added from the second vessel through the first, and the autoclave pressure was increased to 300 psig with argon. The reaction temperature was maintained at 200 °C throughout the experiment. At preselected intervals 7-mL samples were withdrawn through the sampling tube and analyzed as described above under rate studies. The results for DCB monomer and dichloro oligomers are displayed in Figures 2 and 3 and are the averages of three experiments. Not shown are the experimentally found concentrations of 4-chlorothiophenol and 4-(4-chlorophenylthio)thiophenol. These two intermediates were produced in greater quantities than the dichloro oligomers, but the analytical procedure was unable to quantify their concentrations. Control experiments with synthetic mixtures containing 4-chlorothiophenol showed that the ether extractions in the workup procedure were inefficient, and only 40–80% of the thiophenol was typically detected.

Oligomer Analysis after Polymerization. A commercial Ryton V1 PPS (93.17 g) was exhaustively extracted by CH_2Cl_2 in a Soxhlett apparatus for 48 h. During the last several hours, no material was being extracted, yet GPC analysis of the extracted PPS revealed that some of the low molecular weight material still remained (estimated to be 20–30% of the original amount present). LD-FTMS analysis of the recovered solid extract (yield 3.04 g, 3.26 wt %) showed it to be predominantly PPS cyclic oligomers from the tetramer to the tridecamer. The ^{13}C NMR spectrum of the extract showed resonances characteristic²⁵ of the cyclic tetramer, pentamer, and hexamer (dominant) of PPS. We assume the cyclic oligomers with $n > 5$ all have the same NMR spectrum. GC/MS and GC (doping with 1,4-bis(phenylthio)benzene as an internal standard) analyses provided identification and quantitative analyses of the cyclic tetramer (yield 0.066 g, 0.05 wt %) and pentamer (yield 0.41 g, 0.44 wt %). The amounts of the cyclic hexamer through the tridecamer were determined by HPLC by comparing relative peak areas to those for the cyclic tetramer and pentamer with the assumption that all had the same detector response factors (weight basis) (see Figure 7 for an HPLC chromatogram of an extract that had been percolated through both acid-washed and base-washed aluminas). The primary components in Figure 7 were isolated by preparative HPLC. Figure 8 displays the LD-FTMS spectra of the isolated components confirming their identifications as PPS cyclic oligomers. This combination of analyses indicated that the following amounts of cyclic oligomers were extracted from the PPS: (n values): (4) 0.05, (5) 0.44, (6) 0.22, (7) 0.65, (8) 0.82, (9) 0.38, (10) 0.21, (11) 0.14, (12) 0.10, and (13) 0.05 wt %.

Acknowledgment. We sincerely appreciate the skilled experimental assistance provided by J. B. Allison, J. L. Straw, H. D. Yelton, M. J. Wusik, and K. A. Williams. Expert pioneering instrumental analyses were provided by Dr. D. C. Rohlfing, Dr. S. G. Gharfeh, and Mr. J. D. Wood (high-temperature GPC/FID), Dr. S. G. Gharfeh (HPLC), Dr. C. L. Johlman (LD-FTMS), Mr. C. G. Long (high-temperature GC/MS), and Dr. S. M. Wharry (high-temperature ^{13}C NMR). The project benefited greatly from discussions with Drs. J. Janzen, J. F. Geibel, L. M. Stock, O. H. Decker, P. J. DesLauriers, L. E. Scoggins, R. W. Campbell, and J. F. Bunnett.

Supporting Information Available: Supplementary Figures 1 and 2 (2 pages). Ordering information is given on any current masthead page.

References and Notes

- (1) PPS has been produced commercially since 1973 by Phillips Petroleum Co. under the registered trademark Ryton.
- (2) The insolubility, high strength, and temperature stability of PPS make it an attractive engineering thermoplastic. See: Geibel, J. F.; Campbell, R. W. In *Encyclopedia of Chemical Processing and Design*. Volume 40. Polymers, Polyamides,

- Aromatic to Polymers, Polyvinylchloride*; McKetta, J. J., Cunningham, W. A., Eds.; Marcel Dekker: New York, 1992; pp 94–125.
- (3) Reviews: (a) Geibel, J. F.; Campbell, R. W. In *Comprehensive Polymer Science. Volume 5. Step Polymerization*; Eastmond, G. C., Ledwith, A., Russo, S., Sigwalt, P. Eds.; Pergamon Press: Oxford, 1989; pp 543–560. (b) Lopez, L. C.; Wilkes, G. L. *J. Macromol. Sci., Rev. Macromol. Chem. Phys.* **1989**, C29 (1), 83–151. (c) Fradet, A. *Bull. Soc. Chim. Belg.* **1989**, 98, 635–641.
 - (4) Edmonds, J. T., Jr.; Hill, H. W., Jr. (Phillips Petroleum Co.). U.S. Patent 3 354 129, 1967.
 - (5) Koch, W.; Heitz, W. *Makromol. Chem.* **1983**, 184, 779–792.
 - (6) Koch, W.; Risse, W.; Heitz, W. *Makromol. Chem. Suppl.* **1985**, 12, 105–123.
 - (7) Annenkova, V. Z.; Antonik, L. M.; Vakul'skaya, T. I.; Voronkov, M. G. *Doklady Akad. Nauk SSSR* **1986**, 286, 1400–1403.
 - (8) Annenkova, V. Z.; Antonik, L. M.; Shafeeva, I. V.; Vakul'skaya, T. I.; Vitkovskii, V. Yu.; Voronkov, M. G. *Vysokomol. Soed., Ser. B* **1986**, 28, 137–140.
 - (9) Rajan, C. R.; Ponrathnam, S.; Nadkarni, V. M. *J. Appl. Polym. Sci.* **1986**, 32, 4479–4490.
 - (10) Rajan, C. R.; Nadkarni, V. M.; Ponrathnam, S. *J. Polym. Sci.; Part A: Polym. Chem.* **1988**, 26, 2581–2588.
 - (11) Koschinski, I.; Reichert, K.-H. *Makromol. Chem., Rapid Commun.* **1988**, 9, 291–298.
 - (12) Sergeev, V. A.; Nedelkin, V. I. *Makromol. Chem., Macromol. Symp.* **1989**, 26, 333–346.
 - (13) Park, L. S.; Seo, K. H.; Chang, J. G.; Kwon, Y. H.; Han, S. K.; Cha, I. H. *Polymer (Korea)* **1989**, 13, 866–873. Also presented at the Pacific Basin Polymer Conference, Maui, Hawaii, 1989.
 - (14) Ito, M. M.; Onda, M.; Ona, S.; Inoue, H. *Bull. Chem. Soc. Jpn.* **1990**, 63, 1484–1488.
 - (15) Fahey, D. R.; Ash, C. E. *Macromolecules* **1991**, 24, 4242–4249.
 - (16) Nykolyszak, T.; Fradet, A.; Marechal, E. *Makromol. Chem., Macromol. Symp.* **1991**, 47, 363–370.
 - (17) Stille, J. K. *J. Chem. Ed.* **1981**, 58, 862–866.
 - (18) Manaresi, P.; Munari, A. In *Comprehensive Polymer Science. Volume 5. Step Polymerization*; Eastmond, G. C., Ledwith, A., Russo, S., Sigwalt, P. Eds.; Pergamon Press: Oxford, 1989; pp 11–34.
 - (19) For example: Campbell, R. W. (Phillips Petroleum Co.). U.S. Patent 3 919 177, 1975.
 - (20) Miller, J. *Aromatic Nucleophilic Substitution*; Elsevier Publishing Co.: Amsterdam, 1968.
 - (21) Koschinski, I.; Reichert, K.-H.; Traenckner, H.-J. *Die Angew. Makromol. Chem.* **1992**, 201, 11–21.
 - (22) Ravindranath, K. *Polymer* **1990**, 31, 2178–2184.
 - (23) Flory, P. J. *Principles of Polymer Chemistry*, 1st ed.; Cornell University Press: Ithaca, New York, 1953.
 - (24) Reents, W. D., Jr.; Kaplan, M. L. *Polymer* **1982**, 23, 310–313.
 - (25) Kaplan, M. L.; Reents, W. D., Jr. *Tetrahedron Lett.* **1982**, 23, 373–374.
 - (26) Miller, J.; Parker, A. J. *J. Am. Chem. Soc.* **1961**, 83, 117–123.
 - (27) Cox, B. G.; Parker, A. J. *J. Am. Chem. Soc.* **1973**, 95, 408–410.
 - (28) Campbell, J. R. *J. Org. Chem.* **1964**, 29, 1830–1833.
 - (29) McLaughlin, H. S.; Nauman, E. B. *Chem. Eng. Sci.* **1989**, 44, 2157–2164.
 - (30) Gupta, S. K.; Kumar, A. *Reaction Engineering of Step Growth Polymerization*; Plenum Press: New York, 1987; pp 55–56, 68–71.
 - (31) Differential System Simulator, Version 2 (DSS/2); commercially available from Lehigh University, Whitaker Laboratory 5, Bethlehem, PA 18015.
 - (32) Flory, P. J. *J. Am. Chem. Soc.* **1936**, 58, 1877–1885.
 - (33) Attwood, T. E.; Newton, A. B.; Rose, J. B. *Br. Polym. J.* **1972**, 4, 391–399.
 - (34) Yu, T.-y.; Fu, S.-k.; Ji, C.-g.; Cheng, W.-z. *Polymer* **1984**, 25, 1363–1366.
 - (35) Bulai, A. Kh.; Klyuchnikov, V. N.; Urman, Ya. G.; Slonim, I. Ya.; Bolotina, L. M.; Kozhina, V. A.; Gol'der, M. M.; Kuli-chikhin, S. G.; Beghishev, V. P.; Malkin, A. Ya. *Polymer* **1987**, 28, 1349–1357.
 - (36) Campbell, R. W. (Phillips Petroleum Co.). U.S. Patent 3 867 356, 1975.
 - (37) Kinugawa, A. *Kobunshi Ronbunshu* **1987**, 44, 139–141.
 - (38) Stacy, C. J. *J. Appl. Polym. Sci.* **1986**, 32, 3959–3969.
 - (39) Wade, B.; Abhiraman, A. S.; Wharry, S. M.; Sutherlin, D. M. *J. Polym. Sci., Polym. Phys. Ed.* **1990**, 28, 1233–1249.

MA961015D